FROM THE INSTITUTE OF RADIOPHYSICS (DIRECTOR: PROF. R. SIEVERT), STOCKHOLM, SWEDEN.

INDIVIDUALLY DESIGNED FILTERS IN COBALT 60 TELETHERAPY

by

LENNART SUNDBOM

It is the general intention when using radiation for therapeutic purposes to give a high and homogeneous dose to a certain body volume. The dose outside this volume, on the other hand, should be as low as possible, and in organs sensitive to radiation this is of extreme importance. Different methods are therefore used in an attempt to control the dose distribution in the body. The use of wedge filters is a move in that direction (COHEN et coll. 1960). Isodose diagrams show the effect of such filters although for practical reasons the number of these diagrams has to be limited; this practical limitation is also true, of course, in the case of open beams. The number of diagrams may be reduced by standardizing the conditions in the measurement of the diagrams, e. g. by measuring in a water-equivalent material, by making the surface of the phantom plane and perpendicular to the beam axis, and by using only a limited number of types of wedge filter.

This article deals with the possibilities made available by the use of individually designed filters to gain independence from the effect of body contour and the position in the body of the treatment volume. The filters are mounted

Part of the material was presented at a Meeting of the Nordic Society of Medical Radiology, Lund, 8—10 June 1961. Submitted for publication 21 October 1963.

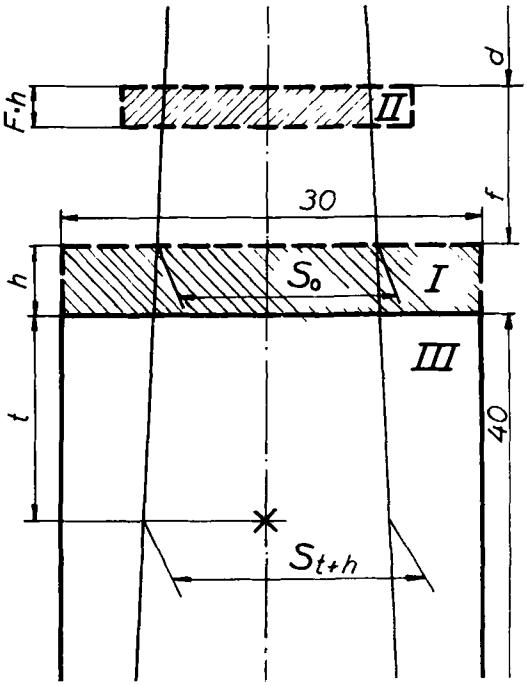

Fig. 1. Measurement arrangement.
I — Mix D block 30 × 30 × h cm
II — Filter 20 × 20 × $F \cdot h$ cm
III — Water phantom 30 × 30 × 40 cm
f — Nominal source-phantom distance
d — Source-filter distance
t — Depth in phantom
h — Thickness of tissue to be replaced by filter
$F \cdot h$ — Thickness of filter
A_{t+h} — Geometrical beam size at $t + h$ cm
A_o — Geometrical beam size at the depth 0.5 cm
In the case of square beams, the sides are marked S_{t+h} and S_o respectively.

at such a distance that the skin-sparing effect of the ^{60}Co γ-radiation will not be destroyed.

The measurements described below have been carried out on one of the ^{60}Co units at Radiumhemmet, an Eldorado Super G unit, produced by the Atomic Energy of Canada Ltd (HULTBERG et coll. 1962). This unit is provided with a block diaphragm, the front of which is situated 35 cm from the source; the source has a diameter of 2 cm.

Basic measurements

A number of basic experiments were performed to investigate the possibilities of calculating the effect of the filter on the distribution of the dose in the body. The measuring arrangements are shown in Fig. 1, which also introduces the symbols used. The measurements were performed with an ionization chamber (BENNER et coll. 1959), the external diameter of which was 4.5 mm and the length 15 mm; the chamber current was amplified by a Vibron electrometer (Model 33 c). The container for the water phantom, of 4 mm perspex, measured 30 × 30 × 40 cm. Blocks of mix D, the thickness of which is marked h, may be placed in front of this phantom; the filter of $F \cdot h$ cm thickness is intended to compensate for the loss of these blocks.

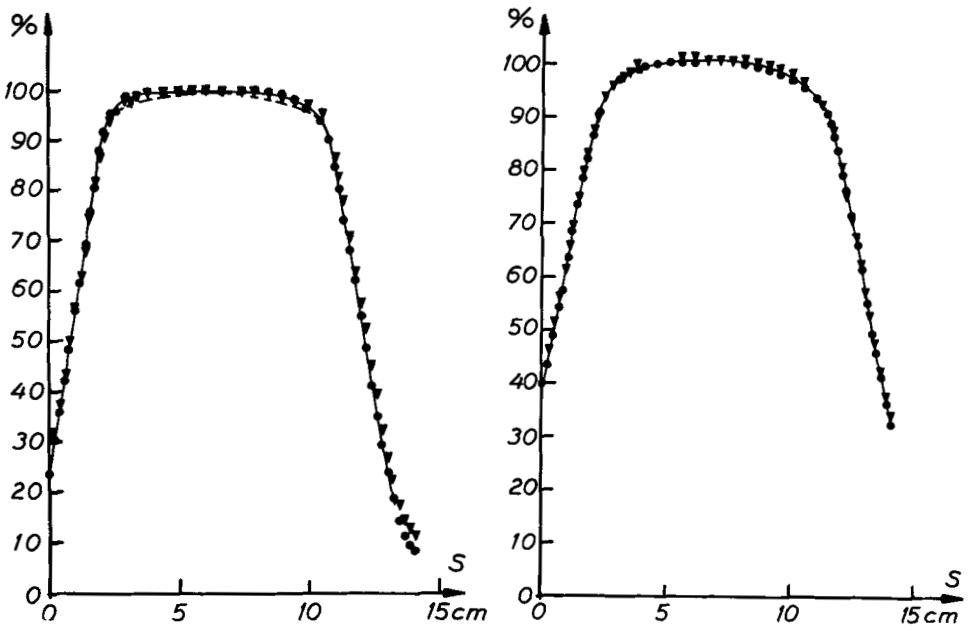

Fig. 2. Dose distribution perpendicular to the beam axis, nominal SPD, *f*, 80 cm, field size A_o, 10 × 10 cm. a) SPD 90 cm, depth in phantom 1 cm. b) SPD 90 cm, depth in phantom 11 cm. ▼ with 6 cm perspex filter at SFD 60 cm, ● open beam, — — — with 10 cm mix D in front of the phantom.

The effect of the filter on the dose perpendicular to the beam axis. The exposure dose for different field sizes was measured along a line perpendicular to the beam axis, firstly with a 6 cm perspex filter at SFD (source-filter distance) 60 cm, and then with only the phantom in the beam, at a source-phantom distance (SPD) of 90 cm. The percentage dose is drawn along a line perpendicular to the beam axis, at depths of 1 and 11 cm, for a field size of 10 × 10 cm (at SPD = 80 cm) in Fig. 2, 100 % being taken to be the dose at the beam axis for $t = 1$ and $t = 11$ cm respectively. Hence, it may be concluded that the filter has no significant effect on the dose distribution within the central part of the beam. A tendency to broadening is found in the distribution curve when the filter is mounted in the beam. A divergence of ± 10 % in the penumbra means a displacement of the curve of only 1 or 2 mm, so that any error introduced in this way, being within the normal tolerances of setting up, may be disregarded in practice. The dose decrease from the beam axis outwards is more rapid for greater depths in the phantom, even though the distance to the source is the same. This is shown by the dotted curve measured along

the above-mentioned line at $t = 1$ cm with 10 cm mix D in front of the phantom. This curve agrees in shape with the one measured at the depth of 11 cm in the cases mentioned first (Fig. 2b). The divergence between the two curves, with and without mix D in front of the phantom, is sufficiently small at the depths used to permit us to limit at least our theoretical studies to a first approximation and to take into account only the dose along the beam axis.

The effect of the filter on the dose along the beam axis. The dose along the beam axis at depths from 1 to 21 cm was measured both with and without a perspex filter in the beam, with the measurement arrangement shown in Fig. 1. The distance from the source to the water phantom was 88 cm, nominal SPD (f) 80 cm, and SFD 60 cm. No mix D block was placed in front of the phantom. With a perspex filter thickness of 5 cm (which was supposed approximately to compensate for a mix D block of 8 cm) the ratio obtained between the doses, with and without filter was:

for field size 5 × 5 cm	1.45
for field size 10 × 10 cm	1.43
for field size 20 × 20 cm	1.37

These measurements were also made with a nominal SPD of 60 cm and a SFD of 40 cm; the distance f—d was thus constant at 20 cm. The maximum deviation in this ratio for any one field size (5 × 5 and 10 × 10 cm) was found by measurements to be less than 2 %. This means that the possible variation of this ratio with different values of f and t compared with the measuring error may be disregarded. The variation according to the field size is significant, and it will be evident from what follows that this variation is advantageous (cf Fig. 6). If the filter is moved closer to the source (increased PFD), the ratio increases. A measurement with the same filter in the beam $A_o = 20 \times 20$ cm and $f = 80$ cm, gave the ratio 1.43 when the filter was mounted at a SFD of 40 cm instead of 60 cm.

All this implies that an effective absorption factor, independent of f and t, can be assumed with a certain thickness of filter. This in narrow beams is relatively independent also of A_o; in the case of broad beams the dose along the beam axis is affected by the position of the filter.

Compensation for irregular body contour

A method of compensation for irregular body contours by use of individually designed filters has been described by Ellis et coll. (1959); the physical basis and the design have been treated by Hall & Oliver (1961). The advantage of this method is that the filter (the compensator) is mounted at a distance (≥ 20 cm) from the patient, as a result of which the skin-sparing effect of the

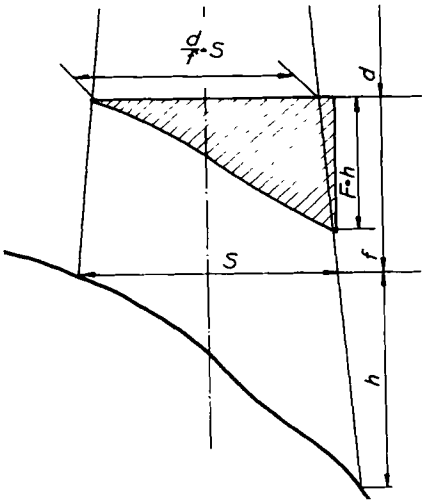

Fig. 3

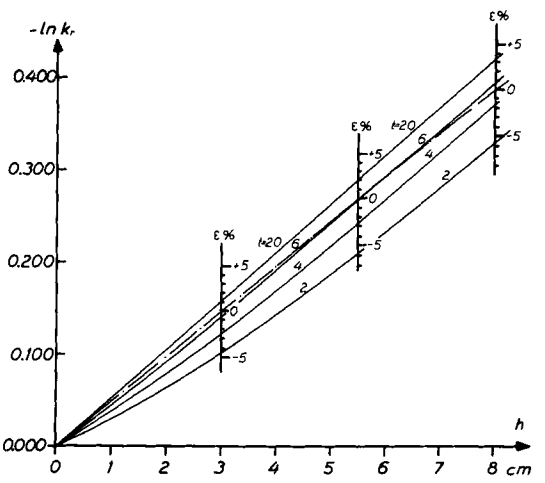

Fig. 4

Fig. 3. Principle of correction for incidence on an irregular body contour.

Fig. 4. Theoretically calculated ideal absorption factor, k_r, as a function of the missing tissue thickness, h, with the depth, t, of tissue as parameter, A_0 10 × 10 cm, ε the error at a constant relation compensator/tissue. The dotted line shows the effective absorption factor of the filter.

^{60}Co γ-radiation is not destroyed, as it is with a tissue-equivalent material (bolus) applied on the skin. Fig. 3 shows the mounting of the filter and the way in which it is dimensioned with regard to the divergence of the beam. The optimum thickness of aluminium filters was calculated by the last-mentioned authors with the formula

$$F \cdot h = \frac{0.88}{\varrho} \cdot h \qquad (1)$$

where ϱ is the density of the filter material.

The aim of the present investigation was to determine the magnitude of the dose divergence obtained by using filters for compensation of body contours and how to make it as small as possible.

There are other methods of dealing with this: Wax compensating blocks may be moulded to fit each individual patient to obtain an artificial surface perpendicular to the beam axis. These blocks are mounted on the diaphragm in order to maintain the skin-sparing effect (COHEN et coll. 1960). Standardized wedge compensators may under certain circumstances be used as described by VAN DE GEIJN (1963). This latter method generally gives a less accurate result than the use of individually designed filters.

Table

Least-square values of power law for tissue-air ratios (new values based on Table 6.5, Brit. J. Radiol. Suppl. 10, 1961)

t, cm	$m(t)$ slope	$100\,K(t)$ intercept	$m(t) - m(0.5)$	$100\,K(t)/K(0.5)$	$1 - m(t)$
0.5	0.01048	97.941	0	100.00	0.98952
1	0.01645	94.336	0.00597	96.32	0.98355
2	0.02275	89.199	0.01227	91.08	0.97725
3	0.02824	84.223	0.01776	85.99	0.97176
4	0.03461	78.993	0.02413	80.65	0.96539
5	0.04124	73.675	0.03076	75.22	0.95876
6	0.04717	69.080	0.03669	70.53	0.95283
7	0.05384	63.597	0.04336	64.93	0.94616
8	0.06058	58.666	0.05010	59.90	0.93942
9	0.06704	54.145	0.05656	55.28	0.93296
10	0.07368	49.867	0.06320	50.92	0.92632
11	0.07905	46.194	0.06857	47.16	0.92095
12	0.08549	42.532	0.07501	43.43	0.91451
13	0.09126	39.207	0.08078	40.03	0.90874
14	0.09671	36.294	0.08623	37.06	0.90329
15	0.10135	33.635	0.09087	34.34	0.89865
16	0.10551	31.276	0.09503	31.93	0.89449
17	0.11019	29.043	0.09971	29.65	0.88981
18	0.11488	26.925	0.10440	27.49	0.88512
19	0.12038	24.825	0.10990	25.35	0.87962
20	0.12557	22.930	0.11509	23.41	0.87443
22	0.13644	19.520	0.12596	19.93	0.86356
24	0.14470	16.741	0.13422	17.09	0.85530
26	0.15192	14.416	0.14144	14.72	0.84808
28	0.16007	12.383	0.14959	12.64	0.83993
30	0.17102	10.485	0.16054	10.70	0.82898

Theoretical calculation of magnitude of error

It was shown under the heading of 'Basic measurements' that only the dose along the beam axis need be considered. This may be obtained from the formula (PFALZNER 1961):

$$\frac{P(f, A_o, t)}{100} = \frac{K(t)}{K(0.5)} \cdot \left(\frac{f + 0.5}{f + t}\right)^{2-2m\,(t)} \cdot A_o{}^{m\,(t)-m\,(0.5)} \tag{2}$$

where $P(f, A_o, t)$ is the percentage dose along the beam axis, whereby 100 % is the dose at depth 0.5 cm.

The values of $K(t)$ and $m(t)$ are evident from the Table, as mentioned by PFALZNER (1962).

The symbols employed are shown in Fig. 1. With the aid of the filter (II) the dose along the beam axis is to be made as similar as possible to the one predominant when the mix D block is mounted in front of the phantom (III).

The percentage depth dose with the block of mix D placed in front of the phantom is:

$$\frac{P_I}{100} = \frac{P\,(f, A_o, t + h)}{100} = \frac{K(t + h)}{K(0.5)} \cdot \left(\frac{f + 0.5}{f + t + h}\right)^{2-2m\,(t+h)} \cdot A_o{}^{m(t+h)-m(0.5)} \tag{3}$$

The percentage depth dose without mix D block and filter is:

$$\frac{P_{II}}{100} = \frac{P(f+h, A_o \cdot \frac{f+h+0.5}{f+0.5}, t)}{100} =$$

$$= \frac{K(t)}{K(0.5)} \cdot \left(\frac{f+h+0.5}{f+h+t}\right)^{2-2m(t)} \cdot A_o{}^{m(t)-m(0.5)} \cdot \left(\frac{f+h+0.5}{f+0.5}\right)^{2m(t)-2m(0.5)} \quad (4)$$

For comparison between the doses, it is assumed that if $P_I = D_I$, then P_{II} should be multiplied by a factor corresponding to the decrease of the intensity of the beam in air. The SPD changes from f to $f + h$ so that

$$D_{II} = P_{II}\left(\frac{f+0.5}{f+h+0.5}\right)^2 \quad (5)$$

The quotient of the backscatter factors for these relatively small variations in field size is not taken into account as it varies by only about 0.2 %.

The error is defined as

$$\varepsilon = \frac{kD_{II} - D_I}{D_I} \quad (6)$$

where k is the effective absorption factor of the filter. The error is zero if

$$k = \frac{D_I}{D_{II}} \quad (7)$$

This value of k, which thus is the ideal one, is marked k_r.
From (6) and (7) we get:

$$\varepsilon = \frac{k}{k_r} - 1 \quad (8)$$

From (3), (4), (5) and (7) we obtain:

$$\tfrac{1}{2}\ln k_r = \tfrac{1}{2}\ln K(t+h) - \tfrac{1}{2}\ln K(t) + [m(t+h) - m(t)]\cdot\ln(f+t+h) + [m(0.5)]\cdot\ln(f+h+0.5) +$$
$$+ [m(t) - m(t+h) - m(0.5)]\cdot\ln(f+0.5) + \tfrac{1}{2}[m(t+h) - m(t)]\cdot\ln A_o \quad (9)$$

The influence of the source-skin distance on the ideal absorption factor (k_r). From (9), if all the variables except f are constant, we obtain the quotient between k_{r1} (at f_1) and k_{r2} (at f_2)

$$\tfrac{1}{2}\ln\frac{k_{r1}}{k_{r2}} = [m(t+h) - m(t)]\cdot[\ln(f_1+t+h) - \ln(f_2+t+h)] + [m(0.5)]\cdot[\ln(f_1+h+0.5) -$$
$$- \ln(f_2+h+0.5)] + [m(t) - m(t+h) - m(0.5)]\cdot[\ln(f_1+0.5) - \ln(f_2+0.5)] \quad (10)$$

If 50 cm $\leq f \leq$ 100 cm, 2 cm $\leq t \leq$ 20 cm and $0 \leq h \leq$ 10 cm, this quotient is constant within 1 or 2 %.

As an example, for h = 8 cm, 2 cm $\leq t \leq$ 22 cm, A_o = 10 × 10 cm and f_1 = 80 cm, the difference between k_{r1} and k_{r2} for f_2 = 60 cm and 100 cm, respectively, is approximately 0.5 %.

The influence of the nominal field size (A_o) *on the ideal absorption factor* (k_r). From (9) we obtain the quotient between k_{r1} (at A_{o1}) and k_{r2} (at A_{o2}):

$$\ln\frac{k_{r1}}{k_{r2}} = [m(t+h) - m(t)]\,[\ln A_{o1} - \ln A_{o2}] \quad (11)$$

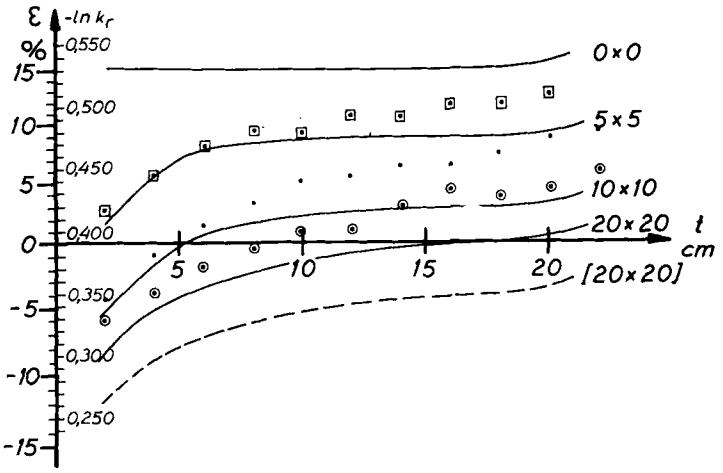

Fig. 5. The theoretically calculated ideal absorption factor, k_r, and the error, ε, respectively as a function of the tissue depth, t, with the nominal field size (at f) as a parameter. The curve for field size 20 × 20 cm is moved + 4 %. Experimental values at nominal field sizes ⊡ 5 × 5 cm, · 10 × 10 cm, ⊙ 20 × 20 cm.

When $h = 8$ cm, and $t = 2$, 12 and 22, respectively, k_{r1} and k_{r2} differ, when $A_{o1} = 5 \times 5$ cm, and $A_{o2} = 20 \times 20$ cm, by 15, 12 and 10 %, respectively. An error of this magnitude is verified in the following (Fig. 6).

The influence of the phantom depth (t) *on the ideal absorption factor* (k_r). Eq. (3) may be written:

$$K(t+h) = \frac{P(f, A_o, t+h)}{100} \cdot K(0.5) \cdot \left(\frac{f+t+h}{f+0.5}\right)^{2-2m(t+h)} \cdot A_o^{-m(t+h)+m(0.5)} \qquad (12)$$

Thus

$$K(t) = \frac{P(f, A_o, t)}{100} \cdot K(0.5) \cdot \left(\frac{f+t}{f+0.5}\right)^{2-2m(t)} \cdot A_o^{-m(t)+m(0.5)} \qquad (13)$$

If (12) and (13) are inserted in (9) we get:

$$\ln k_r = \ln P(f, A_o, t+h) - \ln P(f, A_o, t) + 2[1 - m(t)] \cdot [\ln(f+h+t) - \ln(f+t)] + 2m(0.5)\,[\ln(f+h+0.5) - \ln(f+0.5)] \qquad (14)$$

$P(f, A_o, t+h)$ and $P(f, A_o, t)$ may be read off directly from a depth dose table without interpolation for A_o and f. The depth dose values used in the following have been taken from the British Journal of Radiology (Suppl. No. 10, 1961). In Fig. 4, $\ln k_r$ is drawn as a function of h, with t as a parameter, at the field size (A_o) of 10 × 10 cm.

According to 'Basic measurements' the effective absorption factor of the filter may be written

$$k = e^{-\mu F h} \qquad (15)$$

when $f - d$ is constant; (μ is for broader beams a function of A_o); $\ln k = -\mu\, Fh$, implies a straight line in the diagram in Fig. 4.

From (8) and (15) we obtain:

$$\ln(\varepsilon + 1) = -\mu \cdot Fh - \ln k_r \qquad (16)$$

We put $F \cdot \mu = 0.0482$ (deduced in the following), so that the error may be drawn into the diagram. This has been carried out when $h = 3.0$, 5.5 and 8.0 cm. It will be seen from the diagram that the error when t is less than, or equal to 5 cm (approximately), is relatively independent of the tissue thickness that is to be compensated for when this is 3 cm or more.

In Fig. 5, $ln\ k_r$ has, in accordance with (14), been set off for $h = 8$ cm as a function of t, with the nominal field size as parameter. These curves have been checked by calculating $ln\ k_r$ with tissue/air ratios (Brit. J. Radiol. Suppl. No 10, 1961). Tissue/air ratios are defined:

$$T(S_t, t) = \frac{1}{100} P(f, S_o, t) \cdot B(S_o) \left(\frac{f + t}{f + 0.5}\right)^2 \tag{17}$$

where B is the backscatter factor.

Then with symbols of Fig. 1:

$$P_I = 100 \cdot T\left(S_o \cdot \frac{f + h + t}{f + 0.5}, t + h\right) \cdot \left(\frac{f + 0.5}{f + h + t}\right)^2 \cdot \frac{1}{B(S_o)} \tag{18}$$

$$P_{II} = 100 \cdot T\left(S_o \cdot \frac{f + h + t}{f + 0.5}, t\right) \cdot \left(\frac{f + h + 0.5}{f + h + t}\right)^2 \cdot \frac{1}{B\left(S_o \cdot \frac{f + h + 0.5}{f + 0.5}\right)} \tag{19}$$

P_I and P_{II} are inserted in (7)

$$k_r = \frac{D_I}{D_{II}} = \frac{P_I}{\left(\frac{f + 0.5}{f + h + 0.5}\right)^2 \cdot P_{II}} \approx \frac{T\left(S_o \frac{f + h + t}{f + 0.5}, t + h\right)}{T\left(S_o \frac{f + h + t}{f + 0.5}, t\right)} \tag{20}$$

The agreement between (14) and (20) is very good. The formula (9) varies by a small percentage compared with (20) at greater depth, which is the reason why (14) is inserted instead of (9). The curve for the field size 20 × 20 cm has with regard to ε been moved + 4 %, because of the fact that the effective absorption factor of the filter is less there than at the smaller fields. Eq. (20) has also been deduced by Du Sault & Légaré (1963).

Calculation of the ideal quotient (F) between the thickness of the compensator and that of the compensated tissue

According to (16) and (20) the error follows the function:

$$ln\,(\varepsilon + 1) = -\mu\, Fh - ln\ k_r = -\mu\, Fh - ln \frac{T\left(S_o \cdot \frac{f + h + t}{f + 0.5}, t + h\right)}{T\left(S_o \cdot \frac{f + h + t}{f + 0.5}, t\right)} \tag{21}$$

This means that for a certain value of h and μ, F may be chosen so that the maximum error at a variation of t and A_o is situated symmetrically about zero. We have elected to put $h = 8$ cm, which is a reasonable value for these calculations, although in practice it might sometimes be larger. It is suitable to put $\varepsilon = 0$ at $t = 5$ cm for the field size 10 × 10 cm; the error will then, in most practical cases, be situated within ± 10 % (Fig. 5).

$$\therefore\ \mu\, Fh = 0.390 \tag{22}$$

We define F^1:

$$F = \frac{F^1}{\varrho} \tag{23}$$

where ϱ g/cm^3 = density of compensator material.

$$\therefore \mu\frac{F^1}{\varrho}\cdot h = 0.390 \tag{24}$$

but $\frac{\mu}{\varrho}$ = the effective mass absorption coefficient = μ_m cm²/g.

$$F^1\mu_m\, h = 0.390 \tag{25}$$

According to MORGAN & CORRIGAN (1955) the mass absorption coefficient at 1.25 MeV is: for water 0.0629 cm²/g, for aluminium 0.0546 cm²/g, and for brass 0.052 cm²/g.

$$\left.\begin{aligned} \text{Hence } F^1_{H_2O} &= 0.77 \text{ g/cm}^3 \\ F^1_{Ae} &= 0.89 \text{ g/cm}^3 \\ F^1_{brass} &= 0.94 \text{ g/cm}^3 \end{aligned}\right\} \tag{26}$$

According to HALL & OLIVER (1961) the error is within ± 5 % "for a range of field sizes and values of h" when $F^1_{Al} = 0.88$ g/cm³. This value of F^1_{Al} agrees with (26). The present investigation, however, shows that the error is greater than ± 5 % for depths from 1 to 22 cm, when $h = 8$ cm. According to the same authors, the density of the compensator material is to be

$$\varrho_o = 0.88\frac{f}{d} \tag{27}$$

for the smallest error caused by radiation geometry.

$$\begin{aligned} \text{When } f = 80 \text{ cm and } d = 60 \text{ cm is } \varrho_o &= 1.17 \text{ g/cm}^3 \\ f = 60 \text{ cm and } d = 40 \text{ cm is } \varrho_o &= 1.32 \text{ g/cm}^3 \end{aligned} \tag{28}$$

This is one of the reasons why perspex of 1.18 g/cm³ density has been chosen as compensator material in this investigation. The linear absorption coefficient for perspex is put:

$$\mu_p = \varrho_p\mu_{H_2O} = 1.18\cdot 0.0629 = 0.0742 \text{ cm}^{-1} \tag{29}$$

$$\mu_p \text{ is inserted in (22) to produce } F_p = 0.65 \tag{30}$$

For perspex the value 0.88 in (27) is to be changed to 0.77 and thus $\varrho_o = 1.03$ g/cm³ and 1.16 g/cm³ for $f = 80$, $d = 60$ cm and $f = 60$ cm, $d = 40$ cm respectively (cf. (28)).

Measurements of the error

The dose (D_1) has been measured by the aid of the same ionization chamber as in 'Basic measurements' at certain points along the beam axis in the water phantom; in front of this tissue-equivalent material (mix D) of h cm thickness was mounted at a nominal distance to the source. The mix D block was then removed and replaced by a perspex filter, 0.65 × h cm thick, and the dose (D_2) was measured at the same points (Fig. 1). The values of the error obtained,

$$\varepsilon = \frac{D_2 - D_1}{D_1} \tag{31}$$

are found in Fig. 5.

The theoretical calculations are thus more or less verified. The error increases at greater depths, however, by more than is expected. To adapt the error function to the measured values, the formula (20) has been modified by applying tissue/air ratios for the beam size at the nominal SPD instead of tissue/air ratios for the beam size at the actual depth:

$$ln\, k_r = ln\, T(S_o, t + h) - ln\, T(S_o, t) \tag{32}$$

The values of $ln\, k_r$ thus calculated are inserted in (16) and we obtain

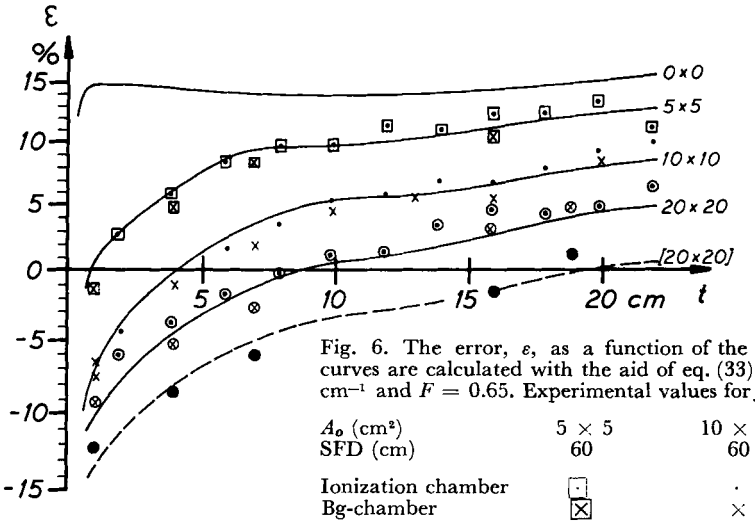

Fig. 6. The error, ε, as a function of the depth in tissue, t. The curves are calculated with the aid of eq. (33), $h = 8$ cm, $\mu = 0.0742$ cm^{-1} and $F = 0.65$. Experimental values for $f = 80$ and $h = 8$ cm:

A_o (cm^2)	5 × 5	10 × 10	20 × 20	
SFD (cm)	60	60	60	40
Ionization chamber	⊡	·	⊙	
Bg-chamber	⊠	×	⊗	●

$$ln\ (\varepsilon + 1) = -\mu\, Fh - ln\ T(S_o, t + h) + ln\ T(S_o, t) \qquad (33)$$

This function is illustrated in Fig. 6 in which $h = 8$ cm, SFD = 60 and 40 cm respectively and $\mu = 0.0742$ cm^{-1}.

The curve for the field size 20 × 20 cm has been moved + 4 % because of the smaller effective absorption factor of the filter. It is evident that agreement with the measured values is very good.

Careful measurements were performed with the so-called Bg-chambers, with an external diameter of 0.5 cm and a length of 2 cm, to check that in the above measurements no systematic error had been present. The measurement accuracy with these chambers is considerable and the wavelength dependence is small, as has been shown by SIEVERT (1934), SKÖLDBORN (1959) and by DAHL and VIKTERLÖF (HULTBERG et coll. 1959). The water phantom was replaced by mix D blocks with holes drilled for the chambers. At the same time the result in 'Basic measurements' was also checked by measurements beside the beam axis out to 1 cm from the field limit. The variations of the measured values at the same depth lie within 2 %. The average values for all the points at any one depth have therefore been inserted in Fig. 6. As can be seen, the agreement is good. The lowest black points are measured with the compensator moved 20 cm closer to the source, and these points are to be found on the curve calculated from (33) when μ is 0.0742 (the same μ as for the field size 10 × 10 cm and the ordinary SFD). This was expected from the results recorded under the heading 'Basic measurements'.

A number of measurements were performed at the nominal source-phantom distances of 60 and 100 cm respectively (SFD 40 and 80 cm respectively). No significant divergence from the corresponding values when $f = 80$ cm was found. Furthermore, when $f = 80$ cm the size of the error was measured for $h = 3.0$ and 5.5 cm respectively. The measured values, compared to the theoretical ones, are again within the limits of error of the measurements.

The variation of the error perpendicularly to the beam axis were measured by the aid of Bg chambers when $f = 100$ cm, $A_o = 10 \times 10$ cm and $h = 8$ cm, the chambers being placed in the beam axis and 5 and 10 cm away from it; the SFD were 80, 60 and 40 cm, respectively. The errors measured when $t = 1.0$, 5.5 and 16.0 cm are given in Fig. 7. It is evident that (33) is not applicable close to the edge of the beam or outside it. The dose 10 cm from the beam

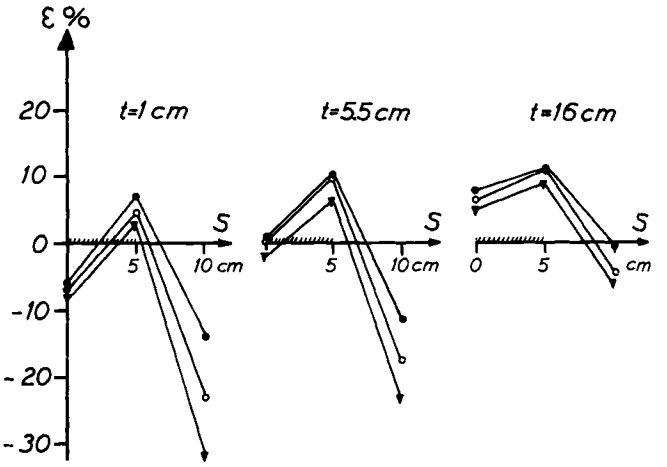

Fig. 7. The size of the error perpendicularly to the beam axis: $f = 100$ cm, $A_o = 10 \times 10$ cm, $h = 8$ cm, $t = 1.0$, 5.5, and 16.0 cm respectively, and distances to beam axis, $s = 0.0$, 5.0 and 10.0 cm, respectively. ● SFD 80 cm, ○ SFD 60 cm, ▼ SFD 40 cm.

axis is lower with the filter in the beam than with mix D on the phantom surface. The figure also shows the variation of the error with SFD, due to the variation in the 'effective absorption coefficient'.

Complete dose distribution at an angle of incidence of 45°

A standard isodose diagram was measured in the water phantom for an open beam, SSD = 80 cm, $A_o = 10 \times 10$ cm with the aid of an automatic isodose recorder (LARSSON et coll. 1963). An ionization chamber of the same type as used in the basic measurements was used as detector but with an exterior diameter of 2.1 mm. These 'standard' isodose curves were compared with those measured at an angle of incidence of 45° with a perspex compensator. The compensator is constructed of perspex columns with a base area of 1.5 × 1.5 cm and mounted at SFD 60 cm, as can be seen in Fig. 8, from which it is evident that the correspondence between the isodose curves is good. The variation of the tilt of the isodose curves with depth agrees with the results shown in Fig. 6, as has earlier been pointed out by MURISON & HUGHES (1957).

Comments on the magnitude of the error

In judging the magnitude of the error one must bear in mind the fact that the error, without compensation, in case of a missing tissue thickness of 8 cm, amounts to between + 30 and + 70 %. If exactitude is desired, the thickness of the compensator may be determined with the aid of (33) and $\mu_p = \mu_{p'}$ (A) by putting $\varepsilon = 0$.

$$F \cdot h = \frac{1}{\mu_p(A)} \cdot [ln\ T(A_o, t) - ln\ T(A_o, t+h)] \tag{34}$$

Example: For a field size of 10 × 10 cm ($\mu_{p'} = 0.0742$) the perspex thickness

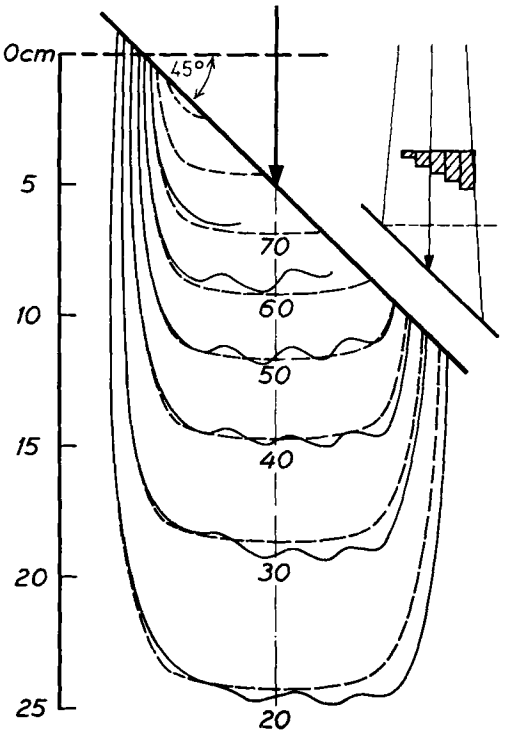

Fig. 8. Example of dose distribution at an incidence of 45° with a compensator constructed of perspex columns, the filter being mounted as shown in the inset section. The continuous curves are measured after compensation while the dotted curves show the standard isodose diagram. SSD = 80 cm, SFD = 60 cm, A_o = 10 × 10 cm.

($F \cdot h$ cm), which gives an error not exceeding 2 or 3 % at a certain depth t, has been set off in Fig. 9 as a function of the tissue thickness, to be compensated (h cm), with the depth ($h + t$ cm) in the standard isodose diagram as a parameter. The use of a constant $F = 0.65$ implies a straight line in the diagram. The error limits $\pm$ 10 % may be drawn in the figure by using this value of F. The curves are to be found almost within these error limits.

The correction method based on multiplication by $e^{\pm \mu_1 h}$ (JOHNS 1961 and GARRETT & JONES 1962), that is to say a factor only dependent on the thickness of the missing tissue, produces the same errors as the compensator method described. This is clear from the fact that multiplication by $e^{\pm \mu_1 h}$, is equivalent to the insertion of a filter, which moderates the beam intensity by $e^{-\mu Fh}$. JOHNS has put $\mu_1 = 0.055$ cm^{-1} which, by compensation according to the above statements, is to be compared to $\mu F = 0.048$ cm^{-1}. It should be observed that the effective absorption factor of the perspex filter varies with the field size in such a way that the error is a little less than if the dose is multiplied by $e^{\pm \mu hF}$ (cf. Fig. 6). The error will become smaller if the entrance point of the beam axis is placed at nominal SSD with the $e^{\pm \mu_1 h}$-method in the example given in Fig. 8.

The physical planning of a radiation treatment is generally made in one

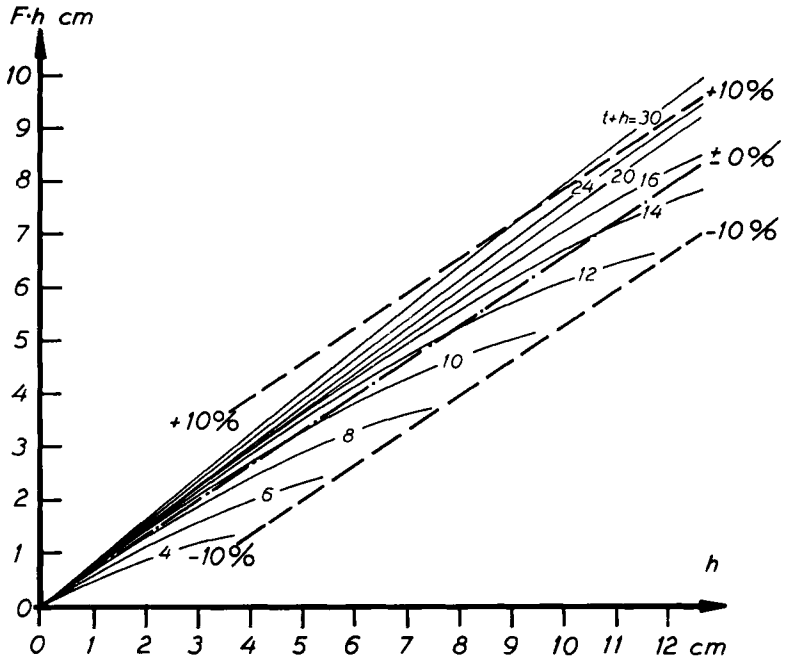

Fig. 9. Diagram for thorough compensation for incidence on an irregular body contour. The thickness of filter, $F \cdot h$, as a function of the tissue thickness which is to be compensated, h, with the depth, $t + h$, in the standard isodose diagram as a parameter. The dotted lines show the error limits $\pm$ 10 % with a constant F.

plane only. If the planes parallel to this plane within the volume subject to the radiation do not have the same shape, or cannot be placed identically with regard to the source, the dose distribution is then not in agreement with that in the calculation plane. This is in many cases a disadvantage which can be eliminated by using a compensator in these cases. It is not always desirable, however, that the dose distribution is reproduced outside the calculation plane and it is necessary in these cases to be able to alter the distribution. This is possible by applying the same principle as in the compensator method, and will be dealt with in the following section.

Modification of standard dose distribution

Fig. 10 represents an example of a radiation treatment in which it is desirable to give the oesophagus a homogenous dose while the spinal cord should get as small a dose as possible. Notwithstanding compensation for the irregular body contour the spinal cord dose in the upper part of the beam is larger than the dose in the lower part of oesophagus. An asymmetrical dose distribution

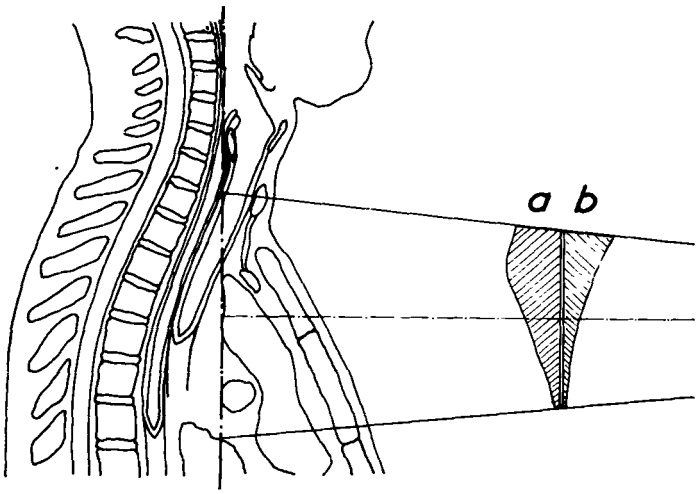

Fig. 10. The principles of compensation for irregular body contour (filter *a*) and for obtaining a homogeneous dose along a certain line in the body (filter *b*).

around the beam axis is desired and this can be brought about by the use of wedge filters (COHEN et coll. 1960). It is of course equally out of the question to measure standard isodose diagrams for every imaginable asymmetric dose distribution, as for every different body contour. The basic arguments presented earlier may be applied in this connection as well.

Theory. An empirical method for the correction of the incidence to irregular body contour has been described by DUTREIX & DUTREIX (1962). This method implies that the isodose curves are to be displaced parallel to the beam axis two-thirds of the distance (h) between the nominal and the actual SSD.

If the beam in Fig. 11 be allowed to fall upon the surface *b*, the dose distribution obtained is equivalent to the displacement to surface *c* of the standard isodose diagram for surface *a*. If the volume between the surfaces *a* and *b* be replaced by a perspex filter, this should have a thickness of 0.65 h, as is clear from the measurements mentioned above. This is approximately 2/3 h, and thus the hypothesis is formed: the isodose curves are displaced parallel to the beam axis at a distance that is equal to the thickness of the perspex filter. This is one reason why perspex has been chosen as compensator material.

Measurements. The measurements were performed in the water phantom with the automatic isodose recorder. The detector (ionization chamber) of the recorder was focused in the beam axis at a certain depth in the phantom, and the ionization current balanced out; a perspex filter was then inserted in the

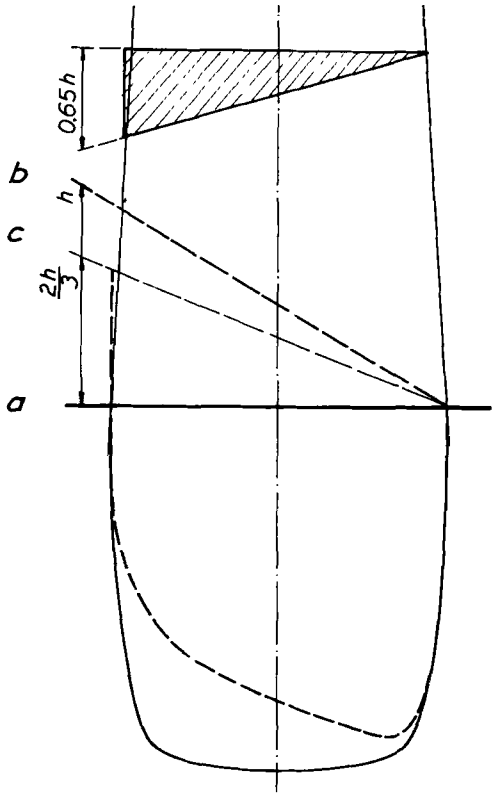

Fig. 11

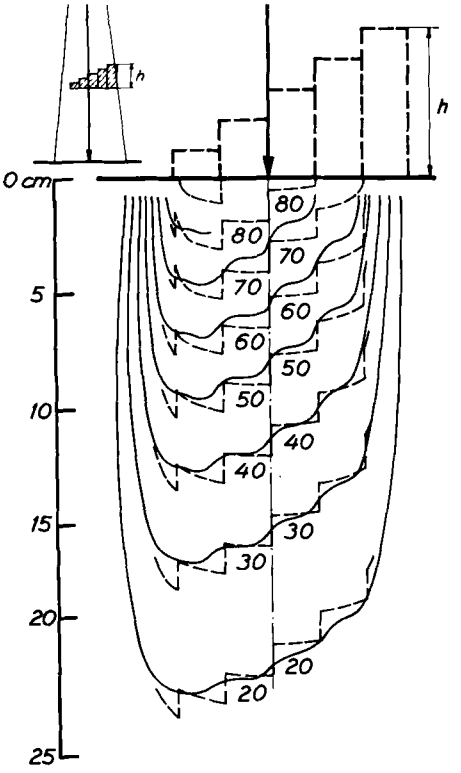

Fig. 12

Fig. 11. The principle of obtaining a homogeneous dose along a certain line. The continuous curve is the standard isodose diagram with no filter and the dotted curve is the standard isodose diagram modified by the filter.

Fig. 12. Example of dose distribution in a modified standard isodose diagram, the filter being mounted as shown in the inset section. Continuous curves are measured, dotted curves are constructed.

beam. The detector moves thereby automatically along the beam axis to a position where the dose rate is the same as in the point from whence it started. The distance between these two positions is subsequently equal to the distance that the isodose diagram is to be displaced. Measurements with field sizes 5×5, 10×10 and 20×20 cm when SSD $= 80$ cm, were performed at depths from 5 to 20 cm, with a filter 5.0 cm thick at SFD $= 60$ cm. The displacement was 5.0 ± 0.2 cm and confirms the validity of the above hypothesis. When measured closer to the surface than 5 cm, the dose is lower than would be expected from the modified standard isodose diagram; for a depth of 0.5 cm the dose is approximately 5 % lower at a displacement of 5 cm. This implies that a dose measured on the incidence surface will seem too low and involve a risk of misinterpretation of the result.

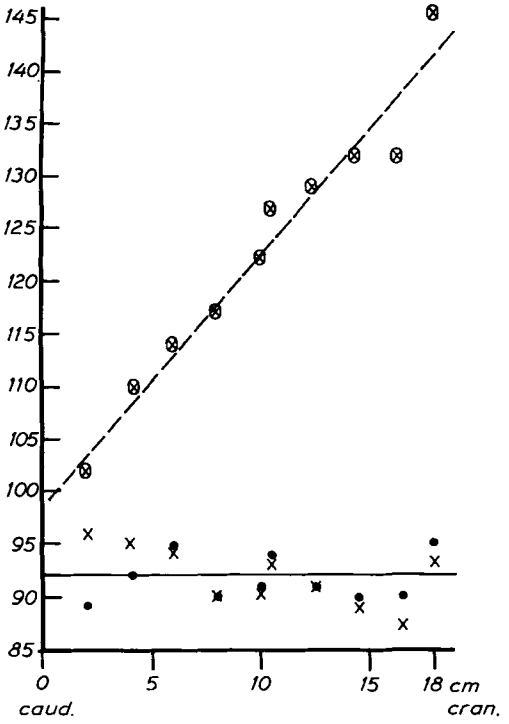

Fig. 13. The dose distribution along the oesophagus, the dose in arbitrary units: ⊗ measured without filter, ● measured with filter according to fig. 10, × calculated for filter according to fig. 10.

Complete dose distribution when the isodoses are displaced at an angle of 55° to the beam axis. The standard isodose diagram (SSD = 80 cm, A_0 = 10 × 10 cm) mentioned earlier has been corrected so that the isodose curves form an angle of approximately 55° to the beam axis. This modified diagram is drawn in Fig. 12. The correction has been made with perspex columns at the phantom surface corresponding to a base area of 2 × 2 cm. Measurements with the aid of the automatic isodose recorder were performed with the filter mounted at SFD 60 cm. It is evident from the figure that there is good agreement between the measured and constructed isodose curves.

Measurements in anatomic phantom by using individually designed filters

The radiation in the oesophagus has been measured with Bg-chambers during the irradiation of a field, SSD = 80 cm and A_0 = 8 × 22 cm, according to Fig. 10; the chambers were positioned in a plastic tube, inserted into the oesophagus. The physically correct anatomic thorax phantom, constructed by DAHL & VIKTERLÖF (1960), was made up of a skeleton and mix D; sawdust

(ϱ = 0.25 g/cm³) was used as a substitute for lung tissue. The irradiation was performed both with and without perspex filters in the beam.

Filter (a) is meant to compensate for the irregular body contour, and is dimensioned according to data given in Fig. 9. The intention is that the error along the oesophagus is to be zero when the filter is in the beam. Filter (b) is used to obtain the same dose along the whole of the oesophagus and is dimensioned according to the above-mentioned hypothesis. The results of the measurements are illustrated in Fig. 13. A dose variation of $\pm$ 20 % has thus been practically eliminated by using two filters.

The dose values, measured without the filters in the beam, have been multiplied by $e^{-\mu_p x}$, where $\mu_p = 0.0742$ cm^{-1} and x = the thickness in cm of the filter passed through by the ray from the centre of the source to the measuring point. The difference between the average of the calculated and of the measured values is 0.2 %. In cases in which intracavitary measurements can be made it may be advantageous to dimension the filter with regard to these. This is especially true in such parts of the body where the beam passes through tissues with absorption greatly differing from that of water.

Conclusions

The dose distribution in the body may be controlled and modified within relatively small error margins with the methods discussed, which may therefore be recommended for practical use. The construction of individual filters is, however, so laborious that there is every reason to try the possibility of adjusting the beams or using standard wedges so as to obtain the desired dose distribution. This has earlier been pointed out by STEWART (1962), but is often not realizable especially in the direction perpendicular to the calculation plane. The individual compensating and beam shaping filters are at present most important for controlling the dose distribution outside the calculation plane and for obtaining predetermined dose distributions.

Acknowledgement

The author wishes to thank Rune Walstam, who suggested the investigation and offered valuable advice during its progress. The work was supported financially by the Cancer Society of Stockholm.

SUMMARY

The author discusses a method of applying ^{60}Co γ-radiation with compensators to adjust for irregular body contours, and with individual filters mounted at a distance of 20 cm or more from the patient to modify the standard dose distributions. The accuracy attained in these cases is treated theoretically and compared to experimental values.

ZUSAMMENFASSUNG

Der Verfasser diskutiert Kobalt 60 Bestrahlung mit Kompensationsfiltern zum Ausgleich von unregelmässigen Körperkonturen sowie die Anwendung von verschiedenen Filtern zur Beeinflussung der Standarddosisverteilungen. Diese Filter sind in einer Entfernung von 20 cm oder mehr von der Oberfläche des Patienten angebracht. Die erhaltene Genauigkeit ist theoretisch berechnet und wird mit gemessenen Werten verglichen.

RÉSUMÉ

L'auteur étudie l'application de la télécobalt-thérapie avec un compensateur adapté à l'irrégularité des contours du corps, et avec des filtres faits spécialement pour chaque malade et montés à une distance de 20 cm ou plus du malade pour modifier la distribution de dose standard. La précision atteinte dans ces cas est calculée théoriquement et comparée aux valeurs expérimentales.

REFERENCES

BENNER S., RAGNHULT I., and GEBERT G.: Miniature ionization chambers for measurements in body cavities. Phys. in Med. Biol. 4 (1959), 26.

COHEN M., BURNS J. E., and SEAR R.: Physical aspects of cobalt 60 teletherapy using wedge filters. I. Physical investigations. II. Dosimetric considerations. Acta radiol. 53 (1960), 401, 486.

DAHL O., and VIKTERLÖF K. J.: Attainment and value of precision in deep radiotherapy. Acta radiol. (1960) Suppl. No. 189.

DEPTH DOSE TABLES FOR USE IN RADIOTHERAPY. Brit. J. Radiol. (1961) Suppl 10.

DU SAULT L. A., and LEGARÉ J.-M.: Dosage calculations for oblique beams of radiation. Radiology 80 (1963), 856.

DUTREIX A., et DUTREIX J.: Construction des isodoses pour les surfaces obliques et irrégulières. J. Radiol. Éléctrol. 43 (1962), 671.

ELLIS F., HALL E. J., and OLIVER R.: A compensator for variations in tissue thickness for high energy beams. Brit. J. Radiol. 32 (1959), 421.

GARRETT J. H., and JONES D. E. A.: Dose distribution problems in megavoltage therapy. II. Obliquity problems in megavoltage therapy. Brit. J. Radiol. 35 (1962), 739.

VAN DE GEIJN J.: Compensation for the effect of oblique incidence of cobalt 60 radiation beams in teletherapy. Brit. J. Radiol. 36 (1963), 56.

HALL E. J., and OLIVER R.: The use of standard isodose distributions with high energy radiation beams. The accuracy of a compensator technique in correcting for body contours. Brit. J. Radiol. 34 (1961), 43.

HULTBERG S., DAHL O., THORAEUS R. et coll.: Kilocurie cobalt 60 therapy at the Radiumhemmet. Acta radiol. (1959) Suppl. 179, p. 89.

— — — — The 4000 curie cobalt 60 therapy installation at Radiumhemmet. Acta radiol. 58 (1962), 1.

JOHNS H. E.: The physics of radiology. Second edition. Charles C. Thomas, Springfield, Ill., 1961.

LARSSON I., LIDÉN K., and STARFELT M.: Automatic isodose recorder. Acta radiol. New Series Therapy Physics Biology 1 (1963), 29.

MORGAN R. H., and CORRIGAN K. E.: Handbook of radiology. The Year Book Publishers, Chicago 1955.

MURISON C. A., and HUGHES H. A.: Physical measurements on a 4-MeV linear accelerator. Radiology 68 (1957), 367.

PFALZNER P. M.: The variation of axial depth dose with focal distance, with field area and with depth. Brit. J. Radiol. 34 (1961), 236.

— New parameters of the power law for tumour-air ratios for Co-60 radiation. Radiology 79 (1962), 439.

SIEVERT R.: Über die Anwendung der Kondensatorkammer für sowohl Röntgen- wie γ-Strahlen-Messungen; zugleich ein Beitrag zu den Vergleichen der biologischen Wirkungen dieser beiden Strahlenarten. Acta radiol. 15 (1934) 193.

SKÖLDBORN H.: On the design, physical properties and practical application of small condenser ionization chambers. Acta radiol. (1959) Suppl. 187.

STEWART J. G.: Dose distribution problems in megavoltage therapy. III. The clinical significance of dose distribution problems. Brit. J. Radiol. 35 (1962), 743.